J Therm Anal Calorim (2010) 99:245–261
DOI 10.1007/s10973-009-0440-6

Thermodynamic property values of selected polycyclic aromatic hydrocarbons measured by differential scanning calorimetry

**Vikram Kestens · Guy Auclair ·
Katarzyna Drozdzewska · Andrea Held ·
Gert Roebben · Thomas Linsinger**

Received: 30 March 2009 / Accepted: 18 August 2009 / Published online: 11 September 2009

Abstract In this study, the use of differential scanning calorimetry (DSC) is demonstrated as a powerful technique that can provide accurate thermodynamic property values of environmental contaminants such as polycyclic aromatic hydrocarbons (PAHs). In total, 47 high purity PAH certified reference materials were selected and analysed by DSC. Their onset melting temperature, enthalpy of fusion and eutectic purity were calculated from the obtained melting endotherms. In addition, the entropy of fusion, which was calculated from the onset melting temperature and enthalpy of fusion, is presented. All measurements were evaluated in a metrologically rigorous manner, including measurement uncertainties.

Keywords Certified reference materials · DSC · Enthalpy of fusion · Melting temperature · Polycyclic aromatic hydrocarbons · Purity · Trueness · Measurement uncertainty

Introduction

Polycyclic aromatic hydrocarbons (PAHs) are a major class of environmental organic contaminants, which includes hundreds of individual substances. All PAHs are represented by a common characteristic skeleton that is made up of carbon and hydrogen atoms and which consists of at least two fused benzene rings. The position and number of these benzene rings and the presence of substituents (N and O) and functional groups (e.g., nitro, alkyl, hydroxyl, amine) strongly define their chemical and physical properties and behaviour. PAHs are derived from both natural and anthropogenic activities. Classical natural sources are volcanic eruptions, forest fires and geological reactions. Anthropogenic contamination might be caused by incomplete combustion of fossil fuels and by a variety of industrial processes such as oil refining, iron and steel production and aluminium casting [1, 2]. As a consequence, PAHs are released to the atmosphere where they tend to adhere to particulate matter [3]. Via aquatic ecosystems and either wet or dry atmospheric deposition, PAHs enter the food chain. Furthermore, PAHs have been linked to adverse health effects, and some of them have been determined to possess mutagenic and/or carcinogenic activities [4–6].

European legislation has been put in place over the years to protect public health and environment from these contaminants [7–11]. Consequently, the levels of PAHs in food, feed and environment need to be regularly monitored. To facilitate the implementation of European legislation concerning PAH monitoring and to support testing laboratories in analytical quality assurance/quality control (QA/QC) including the validation of analytical procedures, the Institute for Reference Materials and Measurements (IRMM) of the Joint Research Centre (JRC) of the European Commission has produced a group of highly pure and well-characterised PAH certified reference materials (CRMs). These CRMs are the basis for the preparation of calibration standards when dissolved in appropriate solvents. The CRM

V. Kestens (✉) · G. Auclair · A. Held · G. Roebben ·
T. Linsinger
European Commission - Joint Research Centre, Institute for
Reference Materials and Measurements (IRMM), Retieseweg
111, 2440 Geel, Belgium
e-mail: vikram.KESTENS@ec.europa.eu

Present Address:
K. Drozdzewska
Institute of Industrial Organic Chemistry, Annopol 6, 03-236
Warsaw, Poland

production activities at the IRMM are accredited according to ISO Guide 34 [12, 13].

As PAHs in the environment occur only as complex mixtures, detection techniques based on chromatographic separation such as GC–MS, GC–FID, HPLC–DAD, HPLC–UV and HPLC–FLD have become the standard techniques for monitoring PAHs in foodstuffs and environmental matrices. However, all techniques have in common a rather tedious, though crucial, sample preparation (clean-up) and analyte recovery step. When sample sizes are limited, analyte enrichment by liquid-phase microextraction (LPME) might be necessary [14]. To develop and improve new and existing methods and to support in vitro and in vivo toxicity evaluation studies, a better understanding of the relations between molecular structures and chemical and physical properties is of utmost importance. This can only be obtained by a combination of complementary analytical techniques, including thermal analysis.

One of the most popular and important thermal analytical techniques is differential scanning calorimetry (DSC). It is a powerful and well-established technique that finds wide applications in the pharmaceutical area and polymer industry [15, 16]. The principle of DSC is based upon measuring the change of the difference in heat flow rate to a sample and a reference sample while they are subjected to a controlled temperature programme [17]. Heat flow changes are caused by chemical reactions (e.g., oxidation, decomposition, etc.) and physical changes (e.g., phase transitions such as melting, crystallisation, glass transitions, etc.).

The aim of this work was to accurately determine the values of a number of thermodynamic properties such as melting temperature and enthalpy and entropy of fusion for a selection of 47 different PAHs by means of DSC tests on highly purified PAH CRMs. In addition, the purity of the PAH CRMs was measured by DSC and compared with their certified purity value in terms of trueness. The purity of 34 of the PAHs was already assessed in a previous study, however, in the current study they have been re-analysed according to ASTM guidelines [18, 19]. All measurement results were evaluated in a metrologically rigorous manner, including uncertainty estimation.

Experimental

Differential scanning calorimetry

Experiments were performed using a Q1000 heat-flux differential scanning calorimeter (TA Instruments-Waters LLC, New Castle, DE, USA). The instrument was purged with a constant flow (50 mL min^{-1}) of high purity (total impurities <0.0005% (m/m)) nitrogen gas (Air Liquide Corp, FR) and cooled by a refrigerated cooling system (TA Instruments-Waters LLC, New Castle, DE, USA). To ensure reliable instrument performance and consistency in measurement results, monthly operation qualification checks were performed.

Calibration

The instrument was calibrated for Tzero$^{\mathrm{TM}}$, temperature and heat (peak transition area). Tzero$^{\mathrm{TM}}$ is a calibration technique patented by TA Instruments-Waters LLC that consists of subsequently heating the empty instrument cell in a first run and α-aluminium oxide (synthetic sapphire) CRM disks, located on both sample and reference position, in a second run. The Tzero$^{\mathrm{TM}}$ calibration allows detection and compensation for instrument imbalances and sample-reference side asymmetry that contribute to instrument baseline heat flow artefacts. A two-point temperature and enthalpy calibration was performed simultaneously by fusion of 2 mg highly pure (>99.999 mol.%) indium (LGC 2601) and tin (LGC 2609) CRM samples in non-hermetically closed aluminium crucibles and a constant heating rate of 1 K min^{-1}. The temperature calibration was based on the determination of the extrapolated peak onset temperatures (T_{e}) for the applied heating rate, followed by a linear extrapolation to zero heating rate ($\beta = 0$). Subtracting T_{e} ($\beta = 0$) from the experimental transition temperature yielded in the temperature calibration factor. The heat (enthalpy) calibration factor was obtained by the ratio of the true heat of fusion and the area enclosed by the transition peak and an interpolated baseline. Both indium and tin CRMs were supplied by LGC (Teddington, UK).

PAH samples

All PAH samples used in these studies were supplied by the IRMM. Sample masses between 0.5 and 2 mg were accurately weighed into standard aluminium crucibles using a microbalance with readability of 0.001 mg. The crucibles were non-hermetically closed using appropriate aluminium lids. An empty crucible and lid of the same type were used as reference. Samples were subsequently equilibrated at a temperature 50 K below their theoretical melting point, isothermally kept during 5 min, and heated through their transition phase with a constant rate of 1 K min^{-1} to approximately 50 K above their melting point.

Onset melting temperature analysis

For each of the tested PAHs, the onset melting temperature (T_{on}) was determined rather than the temperature of the peak maximum (T_{m}). The melting endotherm of pure compounds is very sharp and narrow and therefore, the onset melting temperature can be taken as the melting temperature. In contrast to the peak maximum, the onset melting temperature is independent of the heating rate and the sample mass [20]. The onset melting temperature was determined using the TA Instruments Universal Analysis 2000 software programme.

Purity, enthalpy and entropy of fusion analysis

Purity determination by DSC is based on the fact that impurities lower the melting point of a eutectic system in a predictable way as described by the van't Hoff equation (1).

$$T_{\mathrm{s}} = T_0 - \frac{RT_0^2\chi_2}{\Delta_{\mathrm{fus}H^\circ}}\cdot\frac{1}{F} \qquad (1)$$

where T_{s} is a specific sample temperature, T_0 is the melting temperature of the 100% (mol/mol) pure substance, R is the molar gas constant, χ_2 is the relative sample impurity (mol/mol), $\Delta_{\mathrm{fus}}H^\circ$ is the enthalpy of fusion and F is the melted fraction.

For purity measurements, the sample was heated through its melting range (Fig. 1). The area of the resulting melting endotherm, obtained by integration, corresponds to the enthalpy of fusion. Subsequently, 25 series of fractional areas were selected over a range of 10 to 50% of the total peak area. The fractional areas were then transformed into melted fractions (ratio fractional area to total area). Each melted fraction corresponds to a specific sample temperature.

The van't Hoff linear relationship was graphically presented by plotting the different sample temperatures against the reciprocal of each of their melted fractions. Due to temperature bias between the thermocouple and the true sample temperature, the T_{s} versus $1/F$ curve deviated significantly from the theoretical function. A nonlinear least-squares technique was used to approximate the area increment to correct both the total and each of the fractional areas prior to obtain a straight line. The slope and intercept of the T_{s} versus the corrected $1/F$ curve was obtained by a least-square fit to a straight line (Fig. 2). The sample impurity, obtained from the slope of the curve, was converted into sample purity (=1–impurity).

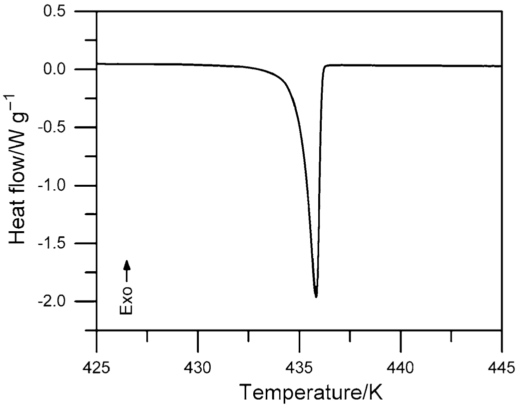

Fig. 1 DSC scan of 3-nitrofluoranthene (BCR-310)

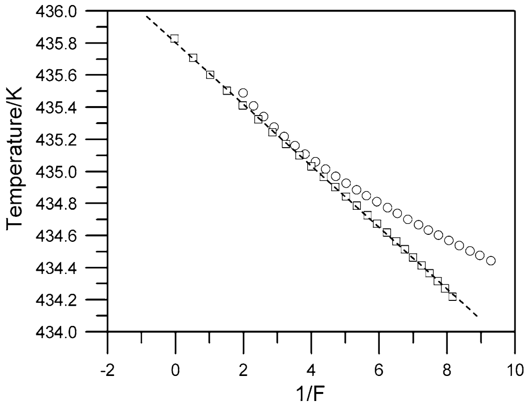

Fig. 2 van't Hoff plot of 3-nitrofluoranthene (BCR-310) before (*circles*) and after (*squares*) linearisation and least-square fit (*dashed line*)

All purity measurements were automatically performed according to the standard ASTM E 928-03 [19] using the TA Instruments Universal Analysis 2000 software programme. The experimental enthalpy of fusion was extrapolated to 100% (mol/mol) purity, resulting in the corrected enthalpy of fusion. Note that only for a minority of the PAHs the experimental and corrected enthalpy deviate by a maximum of 0.1 kJ mol^{-1}. The entropy of fusion was calculated as the ratio of the corrected enthalpy of fusion and onset melting temperature.

Assessment of trueness

Checking the trueness of an analytical method involves estimating its bias. Bias is the difference between the mean value, experimentally determined for the measurand and the accepted true value, for example, the certified value of a CRM [21]. In general, two types of bias can be distinguished. A constant or method bias, independent from the sample matrix and a proportional bias, also called recovery, which is concentration dependent [22]. The latter can only be assessed by analysing CRMs with different levels of the measurands or by spiking studies for different types of matrices. Since only this approach is possible for the materials in question, only a combination of constant bias and proportional bias at the current levels of impurities was determined throughout the study.

To estimate the uncertainty related to the trueness of the enthalpy of fusion and of the melting temperature results, a highly pure indium CRM (LGC 2601) was analysed by DSC under repeatability conditions and compared with its certified enthalpy and certified melting temperature. An overview of the certified values and measurement results is given in Table 1. The certified values were obtained by

Table 1 Certified and measured melting temperature and enthalpy of fusion values for the CRM LGC 2601

	Melting temperature/ °C	Enthalpy of fusion/kJ mol^{-1}
Certified ($x_{\mathrm{CRM}} \pm u_{\mathrm{CRM}}$)	156.61 ± 0.02	3.296 ± 0.009
Measured ($\bar{y}_{\mathrm{m}} \pm u_{\mathrm{m}}$) ($n = 7$)	156.7 ± 0.2	3.28 ± 0.13

adiabatic calorimetry under near equilibrium conditions. All uncertainties shown in Table 1 are expressed as expanded uncertainties ($k = 2$) and correspond to a level of confidence of approximately 95%. The trueness of the DSC purity determination method was estimated from the PAH certified purities and uncertainties as given by the certificates. The PAH certified purity values and associated uncertainties are additionally listed in Table 2. Note that PAH certified purities are expressed in g/g (or mass%), whereas the purities obtained from the DSC method are given in mol/mol (or mol%). It can be assumed that the main organic impurity component mainly consists of isomers of the primary component and intermediates and/or products of side reactions that originate from PAH synthesis and that the molar masses of these organic impurities are not very different from the primary component molar mass. By making this assumption, purities expressed in mass% and mol% can be regarded as being equivalent. The certified purity values were assessed by different analytical techniques such as HPLC–UV, HPLC–FID, GC–MS and direct probe MS, performed during interlaboratory comparison studies. Specific and detailed information concerning the PAH CRMs used in this study can be obtained from the certification reports. These reports can be accessed via the online catalogue on the IRMM website (http://irmm.jrc.ec.europa.eu).

A procedure described in ERM Application Note 1 [23] was used to determine and evaluate the method bias and to asses the uncertainty of trueness for both the melting temperature and enthalpy of fusion results. The procedure consists of different steps. In the first step, the method bias, being the absolute difference between the mean measured value and the certified value, is calculated according to (2).

$$\Delta_{\mathrm{m}}(y) = |\bar{y}_{\mathrm{m}} - x_{\mathrm{CRM}}(y)| \tag{2}$$

where $\Delta_{\mathrm{m}}(y)$ is the method bias, $\bar{y}_{\mathrm{m}}$ is the mean measured value and x_{CRM} is the certified value.

Throughout this article, the symbol “y” indicates the measurement result of measurand “Y”, being either T_{on} and $\Delta_{\mathrm{fus}}H^{\circ}$.

In the second step, the standard uncertainty of the method bias is estimated from the standard measurement uncertainty and the standard uncertainty of the certified value. Both uncertainties are combined using the usual root-sum-of-squares manner, given by (3).

$$u_{\Delta}(y) = \sqrt{u_{\mathrm{m}}(y)^2 + u_{\mathrm{CRM}}(y)^2} \tag{3}$$

where $u_{\Delta}(y)$ is the standard uncertainty of the method bias, $u_{\mathrm{m}}(y)$ is the standard measurement uncertainty and $u_{\mathrm{CRM}}(y)$ is the standard uncertainty of the certified value.

The value of $u_{\mathrm{m}}(y)$ is calculated according to (4).

$$u_{\mathrm{m}}(y) = \frac{s(y)}{\sqrt{n}} \tag{4}$$

where $s(y)$ is the standard deviation and n is the number of replicates.

In the third step, the calculated method bias is evaluated in terms of significance. If one finds $|\Delta_{\mathrm{m}}(y)| \leq U_{\Delta}(y)$, the difference between measurement result and certified value is not significant. The expanded bias uncertainty, $U_{\Delta}(y)$, corresponds to a level of confidence of approximately 95% and is obtained by multiplying $u_{\Delta}(y)$ with a coverage factor, usually equal to 2.

By applying the above described multi-step trueness assessment approach, the method bias calculated from the indium melting temperature and enthalpy of fusion DSC results ($n = 7$) were found not to be significant at a significance level of 5%. As a consequence, the PAH results (Table 2) did not need to be corrected.

Estimation of uncertainty

Repeatability

For each of the PAHs, the DSC method repeatability for onset melting temperature and enthalpy of fusion determinations was investigated. In general, the standard measurement uncertainty of the repeatability, $u_{\mathrm{r}}(y)$, is estimated from (5).

$$u_{\mathrm{r}}(y) = \frac{s(y)}{\sqrt{n}} \tag{5}$$

where $u_{\mathrm{r}}(y)$ is the standard measurement uncertainty of the repeatability, $s(y)$ is the standard deviation and n is the number of replicates.

However, if the number of replicates is insufficient, $u_{\mathrm{r}}(y)$ is not a reliable approximate of $s(y)$. In that case, an additional error would be introduced. Therefore, for all PAHs that were measured in less than seven replicates, $u_{\mathrm{r}}(y)$ was estimated from the standard deviation as a proportion of the mean.

Coverage factor

To ensure that a certain fraction of the possible measurement results can be expected within a defined interval $Y = y \pm U$, the estimated standard combined uncertainty

Table 2 Thermodynamic property values of 47 different PAH CRMs

CAS number of the PAH (CRM code)	Compound name, formula and chemical structure	MW/g mol^{-1}	Onset melting temperature/K $T_{on} \pm U(T_{on})$ (k)	Corrected enthalpy of fusion/kJ mol^{-1} $\Delta_{fus}H° \pm U$ ($\Delta_{fus}H°$) (k)	Entropy of fusion/ J K^{-1} mol^{-1} $\Delta_{fus}S° \pm U$ ($\Delta_{fus}S°$) (k)	Mass fraction/g g^{-1} $\bar{y}_m \pm U(\bar{y}_m)$ ($x_{CRM} \pm U(x_{CRM})$)	n
205-39-0 (BCR-340)	Benzo[*b*]naphtho[*1,2-d*]furan, $C_{16}H_{10}O$ 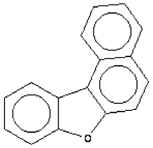	218.25	315.9 ± 0.1 (2.3)	13.7 ± 0.8 (2.3)	43.0 ± 1.5 (4.3)	0.995 ± 0.006 (0.997 ± 0.005)	3
86-57-7 (BCR-306)	1-Nitronaphthalene, $C_{10}H_7NO_2$ 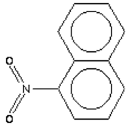	173.17	328.9 ± 0.1 (2.4)	17.3 ± 4.2 (3.8)	52.4 ± 4.8 (4.3)	0.999 ± 0.002 (0.9969 ± 0.0010)	3
195-19-7 (BCR-134)	Benzo[*c*]phenanthrene, $C_{18}H_{12}$ 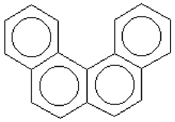	228.29	339.2 ± 0.2 (2.7)	15.5 ± 1.0 (2.4)	45.5 ± 1.8 (4.3)	0.995 ± 0.002 (0.9968 ± 0.0014)	3
581-89-5 (BCR-307)	2-Nitronaphthalene, $C_{10}H_7NO_2$ 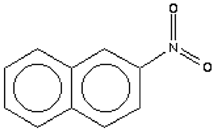	173.17	348.2 ± 0.7 (4.2)	14.5 ± 6.7 (4.1)	41.6 ± 6.9 (4.3)	0.996 ± 0.005 (0.9977 ± 0.0011)	3
132-64-9 (BCR-337)	Dibenzo[*d,b*]furan, $C_{12}H_8O$ 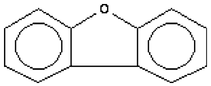	168.19	354.7 ± 0.2 (2.3)	18.6 ± 1.0 (2.3)	52.3 ± 1.8 (4.3)	0.999 ± 0.008 (0.987 ± 0.007)	3

Table 2 continued

CAS number of the PAH (CRM code)	Compound name, formula and chemical structure	MW/g mol^{-1}	Onset melting temperature/K $T_{on} \pm U(T_{on})$ (k)	Corrected enthalpy of fusion/kJ mol^{-1} $\Delta_{fus}H^{\circ} \pm U$ $(\Delta_{fus}H^{\circ})$ (k)	Entropy of fusion/ J K^{-1} mol^{-1} $\Delta_{fus}S^{\circ} \pm U$ $(\Delta_{fus}S^{\circ})$ (k)	Mass fraction/g g^{-1} $\bar{y}_m \pm U(\bar{y}_m)$ $(x_{CRM} \pm U(x_{CRM}))$	*n*
239-30-5 (BCR-341)	Benzo[*b*]naphtho[2,*1*-*d*]furan, $C_{16}H_{10}O$ 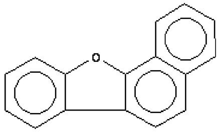	218.25	373.7 ± 0.2 (2.7)	20.9 ± 1.9 (2.7)	55.8 ± 3.0 (4.3)	0.996 ± 0.006 (0.996 ± 0.005)	3
205-43-6 (BCR-137R)	Dibenzo[*b*]naphtho[1,2-*d*]thiophene, $C_{16}H_{10}S$ 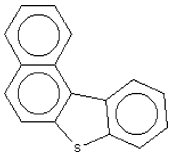	234.32	375.5 ± 0.2 (2.0)	19.0 ± 0.8 (2.0)	50.4 ± 0.8 (2.0)	0.996 ± 0.003 (0.9966 ± 0.0029)	12
225-51-4 (BCR-158)	Benz[*c*]acridine, $C_{17}H_{11}N$ 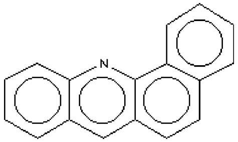	229.28	381.4 ± 0.2 (2.4)	20.3 ± 2.6 (3.0)	53.1 ± 3.6 (4.3)	0.999 ± 0.002 (0.9987 ± 0.0018)	3
3697-24-3 (BCR-81R)	5-Methylchrysene, $C_{19}H_{14}$ 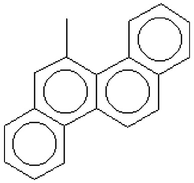	242.32	390.7 ± 0.2 (2.0)	19.0 ± 0.8 (2.0)	48.6 ± 0.8 (2.0)	0.998 ± 0.002 (0.9973 ± 0.0013)	12

Table 2 continued

CAS number of the PAH (CRM code)	Compound name, formula and chemical structure	MW/g mol^{-1}	Onset melting temperature/K $T_{on} \pm U(T_{on})$ (k)	Corrected enthalpy of fusion/kJ mol^{-1} $\Delta_{fus}H° \pm U$ $(\Delta_{fus}H°)$ (k)	Entropy of fusion/ J K^{-1} mol^{-1} $\Delta_{fus}S° \pm U$ $(\Delta_{fus}S°)$ (k)	Mass fraction/g g^{-1} $\bar{y}_m \pm U(\bar{y}_m)$ $(x_{CRM} \pm U(x_{CRM}))$	*n*
194-69-4 (BCR-140)	Benzo[*c*]chrysene, $C_{22}H_{14}$ 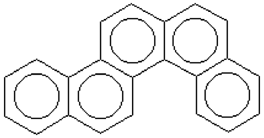	278.35	398.5 ± 0.2 (2.3)	22.7 ± 1.2 (2.3)	56.7 ± 2.2 (4.3)	0.996 ± 0.005 (0.996 ± 0.005)	3
203-12-3 (BCR-139)	Benzo[*g,h,i*]fluoranthene, $C_{18}H_{10}$ 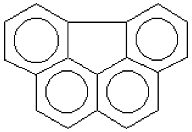	226.27	401.6 ± 0.2 (2.3)	NA	NA	NA (0.995 ± 0.004)	3
225-11-6 (BCR-157)	Benz[*a*]acridine, $C_{17}H_{11}N$ 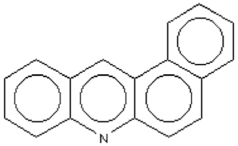	229.28	402.8 ± 0.2 (2.3)	21.9 ± 1.7 (2.5)	54.4 ± 2.9 (4.3)	0.998 ± 0.002 (0.9982 ± 0.0018)	3
116232-62-3 (BCR-342)	Benzo[*a*]fluorenone, $C_{17}H_{10}O$ 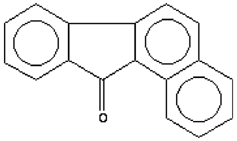	230.27	406.9 ± 0.3 (2.9)	15.6 ± 2.0 (3.0)	38.2 ± 2.8 (4.3)	0.998 ± 0.003 (0.9979 ± 0.0022)	3
602-60-8 (BCR-308)	9-Nitroanthracene, $C_{14}H_9NO_2$ 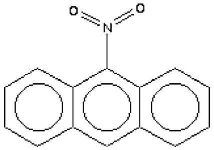	223.23	420.4 ± 0.3 (2.3)	20.1 ± 1.2 (2.3)	47.9 ± 2.2 (4.3)	0.999 ± 0.002 (0.9975 ± 0.0010)	3

Table 2 continued

CAS number of the PAH (CRM code)	Compound name, formula and chemical structure	MW/g mol^{-1}	Onset melting temperature/K $T_{on} \pm U(T_{on})$ (k)	Corrected enthalpy of fusion/kJ mol^{-1} $\Delta_{fus}H° \pm U$ $(\Delta_{fus}H°)$ (k)	Entropy of fusion/ J K^{-1} mol^{-1} $\Delta_{fus}S° \pm U$ $(\Delta_{fus}S°)$ (k)	Mass fraction/g g^{-1} $\bar{y}_m \pm U(\bar{y}_m)$ $(x_{CRM} \pm U(x_{CRM}))$	n
3351-30-2 (BCR-80R)	4-Methylchrysene, $C_{19}H_{14}$ 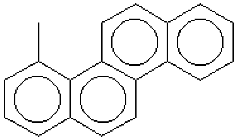	242.32	424.0 ± 0.2 (2.0)	18.3 ± 0.8 (2.0)	43.2 ± 0.8 (2.0)	0.999 ± 0.004 (0.994 ± 0.004)	12
5522-43-0 (BCR-305)	1-Nitropyrene, $C_{16}H_9NO_2$ 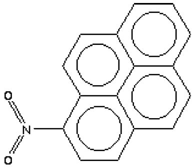	247.25	425.9 ± 0.3 (2.6)	18.9 ± 1.0 (2.3)	44.4 ± 1.6 (4.3)	NA (0.9976 ± 0.0007)	3
194-59-2 (BCR-266)	7*H*-Dibenzo[*c*,*g*]carbazole, $C_{20}H_{13}N$ 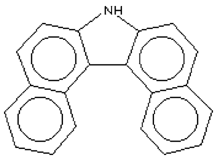	267.32	429.8 ± 0.7 (3.6)	20.1 ± 1.5 (2.5)	46.7 ± 2.6 (4.3)	0.998 ± 0.003 (0.9971 ± 0.0016)	3
1705-85-7 (ERM-AC082)	6-Methylchrysene, $C_{19}H_{14}$ 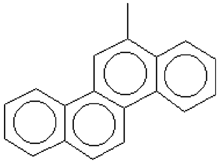	242.32	432.5 ± 0.3 (2.0)	22.7 ± 1.0 (2.0)	52.3 ± 1.0 (2.0)	0.996 ± 0.011 (0.983 ± 0.010)	24

Table 2 continued

CAS number of the PAH (CRM code)	Compound name, formula and chemical structure	MW/g mol^{-1}	Onset melting temperature/K $T_{\mathrm{on}} \pm U(T_{\mathrm{on}})$ (k)	Corrected enthalpy of fusion/kJ mol^{-1} $\Delta_{\mathrm{fus}}H^{\circ} \pm U$ $(\Delta_{\mathrm{fus}}H^{\circ})$ (k)	Entropy of fusion/ J K^{-1} mol^{-1} $\Delta_{\mathrm{fus}}S^{\circ} \pm U$ $(\Delta_{\mathrm{fus}}S^{\circ})$ (k)	Mass fraction/g g^{-1} $\bar{y}_{\mathrm{m}} \pm U(\bar{y}_{\mathrm{m}})$ $(x_{\mathrm{CRM}} \pm U(x_{\mathrm{CRM}}))$	*n*
56-55-3 (BCR-271)	Benz[*a*]anthracene, $C_{18}H_{12}$ 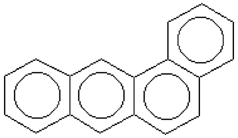	228.29	433.5 ± 0.3 (2.3)	20.1 ± 7.5 (4.1)	46.4 ± 8.0 (4.3)	0.999 ± 0.002 (0.9984 ± 0.0009)	3
892-21-7 (BCR-310)	3-Nitrofluoranthene, $C_{16}H_9NO_2$ 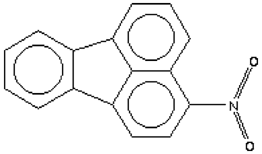	247.25	435.0 ± 0.7 (2.4)	22.6 ± 3.2 (3.1)	51.7 ± 4.3 (4.3)	0.995 ± 0.003 (0.9968 ± 0.0021)	3
193-39-5 (ERM-AC053)	Indeno[1,2,3-*c*,*d*]pyrene, $C_{22}H_{12}$ 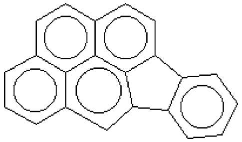	276.33	437.0 ± 0.3 (2.0)	18.6 ± 0.8 (2.0)	42.4 ± 0.8 (2.0)	0.994 ± 0.005 (0.996 ± 0.005)	24
205-82-3 (BCR-49)	Benzo[*j*]fluoranthene, $C_{20}H_{12}$ 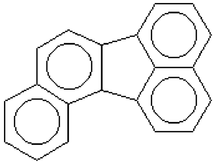	252.31	438.3 ± 0.3 (2.3)	17.9 ± 1.0 (2.3)	40.9 ± 1.6 (4.3)	0.999 ± 0.006 (0.997 ± 0.006)	6

Table 2 continued

CAS number of the PAH (CRM code)	Compound name, formula and chemical structure	MW/g mol^{-1}	Onset melting temperature/K $T_{on} \pm U(T_{on})$ (k)	Corrected enthalpy of fusion/kJ mol^{-1} $\Delta_{fus}H° \pm U$ ($\Delta_{fus}H°$) (k)	Entropy of fusion/ J K^{-1} mol^{-1} $\Delta_{fus}S° \pm U$ ($\Delta_{fus}S°$) (k)	Mass fraction/g g^{-1} $\bar{y}_m \pm U(\bar{y}_m)$ ($x_{CRM} \pm U(x_{CRM})$)	n
205-99-2 (BCR-47)	Benzo[*b*]fluoranthe ne, $C_{20}H_{12}$ 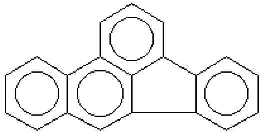	252.31	441.5 ± 0.3 (2.2)	19.6 ± 1.3 (2.7)	44.4 ± 2.9 (4.3)	0.999 ± 0.003 (0.9974 ± 0.0026)	6
5737-13-3 (BCR-338)	4*H*-Cyclopenta[*d*,*e*,*f*]phenanthren-4-one, $C_{15}H_8O$ 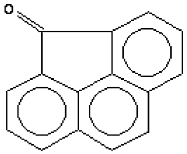	204.22	443.9 ± 0.7 (2.4)	16.3 ± 1.0 (2.3)	36.8 ± 1.9 (4.3)	0.999 +0.001/−0.004 (0.9951 ± 0.0030)	3
3351-31-3 (BCR-79R)	3-Methylchrysene, $C_{19}H_{14}$ 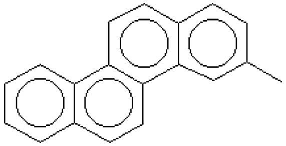	242.32	445.0 ± 0.3 (2.0)	16.5 ± 0.7 (2.0)	37.1 ± 0.7 (2.0)	0.998 ± 0.005 (0.993 ± 0.005)	12
192-97-2 (BCR-50)	Benzo[*e*]pyrene, $C_{20}H_{12}$ 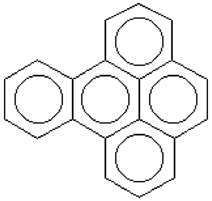	252.31	451.3 ± 0.9 (4.0)	13.8 ± 1.0 (2.5)	30.4 ± 1.7 (4.3)	0.996 ± 0.011 (0.991 ± 0.010)	6

Table 2 continued

CAS number of the PAH (CRM code)	Compound name, formula and chemical structure	MW/g mol^{-1}	Onset melting temperature/K $T_{on} \pm U(T_{on})$ (k)	Corrected enthalpy of fusion/kJ mol^{-1} $\Delta_{fus}H° \pm U(\Delta_{fus}H°)$ (k)	Entropy of fusion/ J K^{-1} mol^{-1} $\Delta_{fus}S° \pm U(\Delta_{fus}S°)$ (k)	Mass fraction/g g^{-1} $\bar{y}_m \pm U(\bar{y}_m)$ ($x_{CRM} \pm U(x_{CRM})$)	n
50-32-8 (ERM-AC051)	Benzo[*a*]pyrene, $C_{20}H_{12}$ 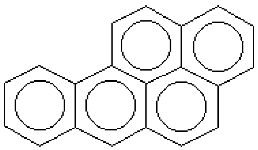	252.31	451.3 ± 0.2 (2.0)	14.7 ± 0.6 (2.0)	32.6 ± 0.6 (2.0)	0.999 ± 0.014 (0.973 ± 0.013)	24
75965-74-1 (BCR-312)	2-Nitro-7-methoxynaphtho[2,*1*-*b*]furan, $C_{13}H_9NO_4$ 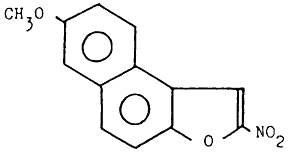	243.23	460.4 ± 0.8 (6.4)	28.7 ± 6.5 (3.7)	62.3 ± 7.5 (4.3)	0.999 ± 0.001 (0.9984 ± 0.0007)	3
217-59-4 (BCR-270)	Triphenylene, $C_{18}H_{12}$ 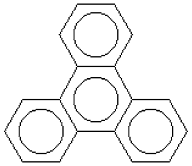	228.29	471.2 ± 0.8 (2.4)	23.0 ± 1.2 (2.4)	48.8 ± 2.1 (4.3)	0.999 ± 0.001 (0.9984 ± 0.0010)	3
215-62-3 (BCR-155)	Dibenz[*a*,*c*]acridine, $C_{21}H_{13}N$ 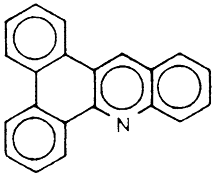	279.34	477.4 ± 0.4 (2.6)	27.8 ± 6.0 (3.7)	58.3 ± 7.0 (4.3)	0.999 ± 0.001 (0.9991 ± 0.0008)	3

Table 2 continued

CAS number of the PAH (CRM code)	Compound name, formula and chemical structure	MW/g mol^{-1}	Onset melting temperature/K $T_{on} \pm U(T_{on})$ (k)	Corrected enthalpy of fusion/kJ mol^{-1} $\Delta_{fus}H° \pm U$ $(\Delta_{fus}H°)$ (k)	Entropy of fusion/ J K^{-1} mol^{-1} $\Delta_{fus}S° \pm U$ $(\Delta_{fus}S°)$ (k)	Mass fraction/g g^{-1} $\bar{y}_m \pm U(\bar{y}_m)$ $(x_{CRM} \pm U(x_{CRM}))$	*n*
226-92-6 (BCR-152)	Dibenz[*a*,*i*]acridine, $C_{21}H_{13}N$ 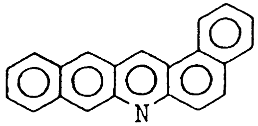	279.34	483.5 ± 0.4 (2.5)	29.6 ± 2.3 (2.5)	61.1 ± 3.8 (4.3)	0.999 ± 0.002 (0.9985 ± 0.0010)	3
7496-02-8 (BCR-309)	6-Nitrochrysene, $C_{18}H_{11}NO_2$ 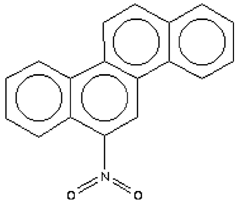	273.29	486.6 ± 0.4 (2.3)	28.4 ± 1.6 (2.3)	58.3 ± 2.9 (4.3)	0.998 ± 0.005 (0.989 ± 0.004)	3
207-08-9 (BCR-48R)	Benzo[*k*]fluoranthene, $C_{20}H_{12}$ 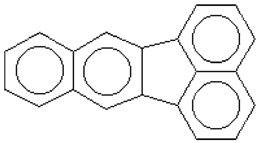	252.31	489.5 ± 0.2 (2.0)	32.4 ± 1.8 (2.3)	66.3 ± 3.3 (4.3)	0.999 +0.001/−0.004 (0.997 ± 0.004)	3
224-42-0 (BCR-154)	Dibenz[*a*,*j*]acridine, $C_{21}H_{13}N$ 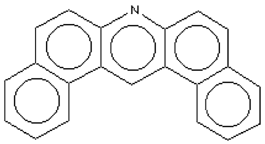	279.33	492.7 ± 0.4 (2.4)	25.5 ± 2.4 (2.7)	51.8 ± 3.8 (4.3)	0.998 ± 0.002 (0.998 ± 0.001)	3
13345-21-6 (BCR-343)	3-Hydroxybenzo[*a*]pyrene, $C_{20}H_{12}O$ 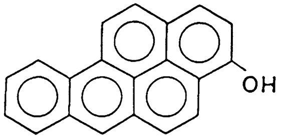	268.32	496.9 ± 0.6 (3.4)	24.1 ± 1.6 (2.4)	48.4 ± 2.9 (4.3)	0.997 ± 0.009 (0.994 ± 0.008)	3

Table 2 continued

CAS number of the PAH (CRM code)	Compound name, formula and chemical structure	MW/g mol^{-1}	Onset melting temperature/K $T_{on} \pm U(T_{on})$ (k)	Corrected enthalpy of fusion/kJ mol^{-1} $\Delta_{fus}H° \pm U$ ($\Delta_{fus}H°$) (k)	Entropy of fusion/ J K^{-1} mol^{-1} $\Delta_{fus}S° \pm U$ ($\Delta_{fus}S°$) (k)	Mass fraction/g g^{-1} $\bar{y}_m \pm U(\bar{y}_m)$ ($x_{CRM} \pm U(x_{CRM})$)	n
226-36-8 (BCR-153R)	Dibenz[*a*,*h*]acridine, $C_{21}H_{13}N$ 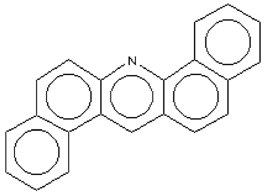	279.33	499.7 ± 0.3 (2.0)	30.6 ± 1.3 (2.0)	61.3 ± 1.3 (2.0)	0.999 ± 0.001 (0.9992 ± 0.0006)	12
5385-75-1 (BCR-265)	Dibenzo[*a*,*e*]fluoranthene, $C_{24}H_{14}$ 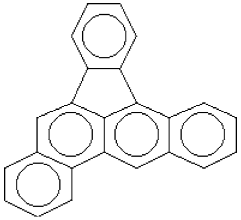	302.37	505.5 ± 0.4 (2.4)	24.0 ± 1.9 (2.5)	47.4 ± 3.2 (4.3)	0.999 ± 0.002 (0.9985 ± 0.0016)	3
192-65-4 (BCR-133)	Dibenzo[*a*,*e*]pyrene, $C_{24}H_{14}$ 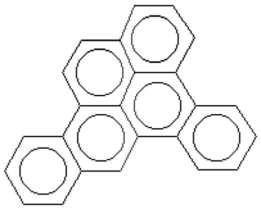	302.37	517.9 ± 1.9 (4.2)	32.1 ± 2.8 (2.7)	61.9 ± 4.6 (4.3)	0.998 ± 0.005 0.996 ± 0.005	3
3074-00-8 (BCR-339)	6*H*-benzo[*c*,*d*]pyren-6-one, $C_{19}H_{10}O$ 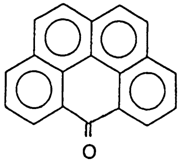	254.29	524.2 ± 1.1 (3.9)	13.1 ± 1.7 (3.0)	25.0 ± 2.3 (4.3)	NA (0.988 ± 0.009)	–

Table 2 continued

CAS number of the PAH (CRM code)	Compound name, formula and chemical structure	MW/g mol^{-1}	Onset melting temperature/K $T_{on} \pm U(T_{on})$ (k)	Corrected enthalpy of fusion/kJ mol^{-1} $\Delta_{fus}H° \pm U$ $(\Delta_{fus}H°)$ (k)	Entropy of fusion/ J K^{-1} mol^{-1} $\Delta_{fus}S° \pm U$ $(\Delta_{fus}S°)$ (k)	Mass fraction/g g^{-1} $\bar{y}_m \pm U(\bar{y}_m)$ $(x_{CRM} \pm U(x_{CRM}))$	n
218-01-9 (BCR-269)	Chrysene, $C_{18}H_{12}$ 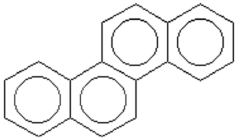	228.29	527.0 ± 1.1 (2.4)	23.6 ± 2.2 (2.7)	44.8 ± 3.5 (4.3)	NA (0.9928 ± 0.0028)	–
63041-90-7 (BCR-311)	6-Nitrobenzo[*a*]pyrene, $C_{20}H_{11}NO_2$ 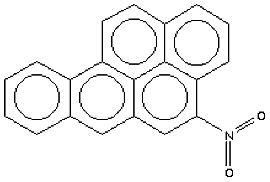	297.31	528.4 ± 0.4 (2.4)	30.2 ± 1.6 (2.3)	57.0 ± 2.9 (4.3)	0.999 ± 0.002 (0.9978 ± 0.0010)	3
53-70-3 (BCR-138)	Dibenz[*a*,*h*]anthracene, $C_{22}H_{14}$ 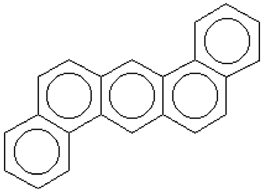	278.35	539.7 ± 0.4 (2.4)	28.4 ± 1.6 (2.3)	52.7 ± 2.9 (4.3)	0.999 +0.001/−0.008 (0.990 ± 0.007)	3
193-43-1 (BCR-267)	Indeno [*1*,*2*,*3*-*cd*]fluoranthene, $C_{22}H_{12}$ 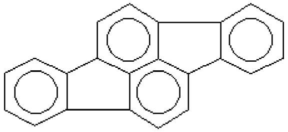	276.33	542.3 ± 0.5 (2.4)	23.2 ± 1.9 (2.6)	42.8 ± 3.2 (4.3)	0.999 +0.001/−0.100 (0.9986 ± 0.0009)	3

Table 2 continued

CAS number of the PAH (CRM code)	Compound name, formula and chemical structure	MW/g mol^{-1}	Onset melting temperature/K $T_{on} \pm U(T_{on})$ (k)	Corrected enthalpy of fusion/kJ mol^{-1} $\Delta_{fus}H° \pm U$ ($\Delta_{fus}H°$) (k)	Entropy of fusion/ J K^{-1} mol^{-1} $\Delta_{fus}S° \pm U$ ($\Delta_{fus}S°$) (k)	Mass fraction/g g^{-1} $\bar{y}_m \pm U(\bar{y}_m)$ ($x_{CRM} \pm U(x_{CRM})$)	n
214-17-5 (BCR-46)	Benzo[*b*]chrysene, $C_{22}H_{14}$ 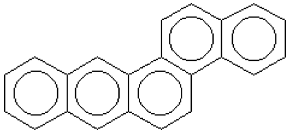	278.35	574.2 ± 0.5 (2.4)	25.3 ± 3.1 (3.0)	44.0 ± 4.4 (4.3)	0.999 +0.001/−0.008 (0.994 ± 0.008)	6
189-64-0 (BCR-159)	Dibenzo[*a*,*h*]pyrene, $C_{24}H_{14}$ 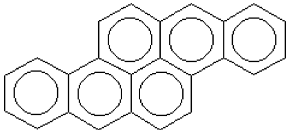	302.37	590.8 ± 0.5 (2.3)	26.9 ± 1.5 (2.3)	45.5 ± 2.7 (4.3)	0.998 ± 0.008 (0.9928 ± 0.0070)	3
213-46-7 (BCR-168)	Picene, $C_{22}H_{14}$ 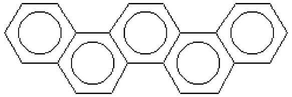	278.35	639.0 ± 0.6 (2.4)	NA	NA	NA (0.998 ± 0.004)	3
191-07-1 (BCR-272)	Coronene, $C_{24}H_{12}$ 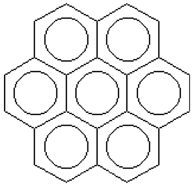	300.35	710.8 ± 0.8 (2.7)	NA	NA	NA (0.9989 ± 0.0006)	3

MW molecular weight; T_{on}, onset melting temperature; $U(T_{on})$, expanded uncertainty of T_{on}; $\Delta_{fus}H°$, standard molar enthalpy of fusion; $U(\Delta_{fus}H°)$, expanded uncertainty of $\Delta_{fus}H°$; $\Delta_{fus}S°$, standard molar entropy of fusion; $U(\Delta_{fus}S°)$, expanded uncertainty of $\Delta_{fus}S°$; $\bar{y}_m$, measured purity; $U(\bar{y}_m)$, expanded uncertainty of $\bar{y}_m$; x_{CRM}, certified purity; $U(x_{CRM})$, expanded uncertainty of x_{CRM}; NA, enthalpy of fusion and/or purity determination was not possible due to melting peak irregularities or decomposition during melting; *n*, number of replicates needs to be expanded by multiplying with a coverage factor [24]. The expanded uncertainty is then given by (6).

$$U = k\, u_c(y) \tag{6}$$

where U is the expanded uncertainty, k is the coverage factor and $u_c(y)$ is the combined uncertainty.

The value of the coverage factor is chosen on the basis of the desired level of confidence associated with the interval defined by U. Typically the coverage factor is in the range 2–3. According to the Central Limit Theorem, a coverage factor of 2 and 3 can be applied to define an interval having a level of confidence of approximately 95 and 99%, respectively. However, this approach is only valid for measurement results that are normally distributed and when $u_c(y)$ is not dominated by a standard uncertainty component from a type A evaluation based on only a few measurement replicates [24].

In this study, many of the average onset melting temperature and enthalpy of fusion DSC results originate from triplicate measurements and thus it can be assumed that, due to the lack of effective degrees of freedom, v_{eff}, $u_c(y)$ cannot be regarded as an appropriate estimate of the standard deviation. Therefore, for all PAHs for which their experimental average melting temperature and enthalpy of fusion results were based on less than seven measurement replicates, an individual coverage factor was calculated based on a t-distribution using a v_{eff} obtained from the Welch–Satterthwaite formula as given by (7).

$$v_{\mathrm{eff}} = \frac{u_c^4(y)}{\sum_{i=1}^{N} \frac{u_i^4(y)}{v_i}} \tag{7}$$

As the calculated v_{eff} values were no integers, the corresponding coverage factors were obtained by interpolation. For all other PAHs, a coverage factor of 2, indicating a level of confidence of approximately 95%, was used.

Combined and expanded uncertainty

The combined uncertainties for T_{on} and $\Delta_{\mathrm{fus}}H^{\mathrm{o}}$ were obtained by combining the standard uncertainties from trueness and repeatability (8).

$$u_c(y) = \sqrt{u_r(y)^2 + u_\Delta(y)^2} \tag{8}$$

One may suggest including uncertainties arising from weighing and sample heterogeneity into the overall uncertainty budget. Indeed, both can be a significant source of uncertainty. However, it can be assumed that they are already covered by the repeatability (for sample heterogeneity) and trueness (for the weighing contribution) uncertainty.

Finally, the expanded uncertainties were calculated by multiplying $u_c(y)$ with their coverage factors.

The combined uncertainties for entropy of fusion, $u_c(\Delta_{\mathrm{fus}}S^{\mathrm{o}})$, were estimated from the standard combined uncertainties of the onset melting temperature, $u_c(T_{\mathrm{on}})$, and the enthalpy of fusion, $u_c(\Delta_{\mathrm{fus}}H^{\mathrm{o}})$. Both were obtained by dividing the expanded uncertainties by their corresponding coverage factors. The combined standard uncertainties were then combined using the root-sum-of-squares manner and again expanded by their coverage factor, resulting into the expanded uncertainties for entropy of fusion, $U(\Delta_{\mathrm{fus}}S^{\mathrm{o}})$.

A complete overview of the experimental results and their uncertainties together with some characteristic information such as the molecular weight and Chemical Abstract Service (CAS) registry number is given in Table 2.

Conclusions

In this study, the onset melting temperature and enthalpy of fusion for a selection of 47 different PAHs were measured by DSC. Subsequently, sample purity and entropy of fusion were calculated and evaluated. For 6 out of the 47 PAHs, purity could not be assessed by means of DSC. The main reasons were decomposition during melting (e.g., chrysene, picene and coronene) and partially unresolved peaks in the melting area (e.g., benzo[*g*,*h*,*i*]fluoranthene and 1-nitropyrene). 6*H*-benzo[*c*,*d*]pyren-6-one showed to be stable before and during melting, however, the heat capacity of the baseline after melting was significantly lower than before melting. Purity assessment could only be done by sigmoidal peak integration instead of a normal linear peak integration. From that point of view, 6*H*-benzo[*c*,*d*]pyren-6-one was regarded as insufficient stable thus excluded for DSC purity determination.

All results originate from at least triplicate measurements carried out under repeatability conditions and are accompanied with an estimated expanded uncertainty. It has to be noted that 34 of the PAHs have already been discussed in a previous article [18]. However, the purity uncertainties were only estimated from the standard deviations from three replicates and the square root of the number of replicates. In this study, all measurement uncertainties are combined uncertainties, taking into account the trueness and repeatability uncertainties. Consequently, the newly estimated measurement uncertainties are larger. In addition, the calculated purity values obtained for the 34 PAHs during the previous study were recalculated according to ASTM E 928-03 guidelines [19]. Recently, the IRMM has reassessed the certified values and uncertainties of many of the PAH CRMs. Some of the certified uncertainties that were previously described as following a triangular distribution have been recalculated according to a level of confidence of approximately 95% ($k = 2$), taking into account the triangular distribution.

Based on the data from the current study, we can conclude that DSC is a powerful technique capable to provide accurate values of thermodynamic properties of environmental contaminants such as PAHs. The bias values obtained during the trueness evaluation study for onset melting temperature and enthalpy of fusion were not significant. Therefore, the DSC methods as described in the current article can be regarded as being capable to give the correct (true) results within a calculable uncertainty. For several PAHs, a significant bias between the measured and certified purity was found. This phenomenon was also observed during the previous study [18]. The purity calculated from DSC results is only valid for eutectic systems, in which case the content of impurities in mol.% can be calculated.

Only impurities which form a eutectic system during melting will be determined. It can be expected that impurities, which form ideal solutions are soluble in the liquid phase and insoluble in the solid state. The formation of solid solutions and pure crystals is based upon the molecular interactions between the impurities and the compound molecules [25]. The probability of the formation of solid solutions is greater for disordered crystals. A measure of the disorder in the solid state is the entropy of fusion. Donnelly et al. [26] observed that organic compounds with an entropy of fusion value below 33.5 J mol^{-1} K^{-1} may form more easily solid solutions with the impurities, resulting into an experimental eutectic impurity, which is higher than its true purity. In the case of PAHs, this implies that inorganic impurities are not detected. From 44 PAH CRMs, which allowed entropy of fusion determination, only 3 (BCR-50, ERM-AC51 and BCR-339) were found to have an entropy of fusion value below 33.5 J mol^{-1} K^{-1}. Among them, ERM-AC51 and BCR-339 have a significant purity bias. As the impurity substance is often not known, the hypothesis of dealing with a eutectic system cannot always be easily checked. In that case, the “DSC purity” shall not be used or reported as SI traceable purity. Instead, and if the absolute accuracy of the test results is important, the DSC purity measurements must be backed up with other analytical techniques. The validity of the DSC purity determination method is currently being further investigated.

References

1. Yang HH, Lai SO, Hsieh LT, Hsueh HJ, Chi TW. Profiles of PAH emission from steel and iron industries. Chemosphere. 2002;48:1061–74.
2. Mi HH, Lee WJ, Chen CB, Yang HH, Wu SJ. Effect of fuel aromatic content on PAH emission from a heavy-duty diesel engine. Chemosphere. 2000;41:1783–90.
3. Moon HB, Kannan K, Lee SJ, Ok G. Atmospheric deposition of polycyclic aromatic hydrocarbons in an urban and a suburban area of Korea from 2002 to 2004. Environ Contam Toxicol. 2006;51:494–502.
4. Weisburger JH. A perspective on the history and significance of carcinogenic and mutagenic N-substituted aryl compounds in human. Mut Res Fund Mol Mech Mut. 1997;376:261–6.
5. White PA. The genotoxicity of priority polycyclic aromatic hydrocarbons in complex mixtures. Mut Res-Gen Tox Env Mut. 2002;515:85–98.
6. Straif K, Baan R, Grosse Y, et al. Carcinogenicity of polycyclic aromatic hydrocarbons. Lancet Oncol. 2005;6:931–2.
7. European Union. Directive 2000/60/EC of the European Parliament and of the Council. Off J Eur Commun. 2000;L 327:1–72.
8. European Union. Directive 2004/107/EC of the European Parliament and of the Council. Off J Eur Commun. 2005;L 23:3–16.
9. European Union. Decision 2455/2001/EC of the European Parliament and of the Council. Off J Eur Commun. 2001;L 331:1–5.
10. European Union. Council Directive 98/83/EC. Off J Eur Commun. 1998;L330:32–54.
11. European Union. Commission Regulation (EC) No. 1881/2006. Off J Eur Commun. 2006;L 364:5–24.
12. ISO Guide 34:2000—General requirements for the competence of reference material producers, ISO, Geneva, Switzerland.
13. Linsinger TPJ, Bernreuther A, Corbisier Ph, et al. Accreditation of reference material producers: the example of IRMM’s Reference Materials Unit. Accred Qual Assur. 2007;12:167–74.
14. Basheer C, Balasubramanian R, Lee HK. Determination of organic micropollutants in rainwater using hollow fiber membrane/liquid-phase microextraction combined with gas chromatography–mass spectrometry. J Chromatogr A. 2003;1016:11–20.
15. Giron D. Applications of thermal analysis and coupled techniques in pharmaceutical industry. J Therm Anal Cal. 2002;68:335–57.
16. Kong Y, Hay JN. The enthalpy of fusion and degree of crystallinity of polymers as measured by DSC. Eur Polym J. 2003;39:1721–8.
17. Höhne G, Hemminger W, Flammersheim HJ. Differential scanning calorimetry: an introduction for practitioners. 1st ed. New York: Springer; 2003.
18. Drozdzewska K, Kestens V, Held A, Roebben G, Linsinger T. Differential scanning calorimetry to measure the purity of polycyclic aromatic hydrocarbons. J Therm Anal Cal. 2007;88:757–62.
19. ASTM 928-03 standard test method for purity by differential scanning calorimetry, ASTM, West Conshohocken, USA.
20. Schawe J. Evaluation and interpretation of peak temperatures of DSC curves. Part 1: basic principles. Mettler Toledo UserCom. 2006;1:6–9.
21. ISO 5725:1994—Accuracy (trueness and precision) of measurement methods and results, part 4: basic methods for the determination of the trueness of a standard measurement method, ISO, Geneva, Switzerland.
22. Maroto A, Boqué R, Riu J, Rius FX. Measurement uncertainty in analytical methods in which trueness is assessed from recovery assays. Anal Chim Acta. 2001;440:171–84.
23. Linsinger T (2005) Application note 1—comparison of a measurement result with the certified value. European Reference Materials. http://www.erm-crm.org. Accessed March 2009.
24. ISO/IEC Guide 98:2008—Uncertainty of measurement, part 3: guide to the expression of uncertainty in measurement (GUM: 1995), ISO, Geneva, Switzerland.
25. Książczak A, Nagata I. Crystal-plastic and plastic-liquid phase transitions, and purity determination. Thermochim Acta. 1995;254:31–9.
26. Donnelly IR, Drewers LA, Johnson RL, Munslow WD, Knapp KK, Sovocool GW. Purity and heat of fusion data for environmental standards as determined by differential scanning calorimetry. Thermochim Acta. 1990;167:155–87.